HHS Public Access

Author manuscript

Acta Biomater. Author manuscript; available in PMC 2017 November 01.

Published in final edited form as:

Acta Biomater. 2016 November ; 45: 234–246. doi:10.1016/j.actbio.2016.08.053.

Accelerated wound healing in a diabetic rat model using decellularized dermal matrix and human umbilical cord perivascular cells

P. Brouki Milan[a], **N. Lotfibakhshaiesh**[a,*], **M.T. Joghataie**[a,b,*], **J. Ai**[a], **A. Pazouki**[c], **D.L. Kaplan**[d], **S. kargozar**[a], **N. Amini**[b], **M.R. Hamblin**[e,f,g], **M. Mozafari**[b,h,i], and **A. Samadikuchaksaraei**[b,i,j]

P. Brouki Milan: peiman.brouki@gmail.com; N. Lotfibakhshaiesh: n.lotfiba@tums.ac.ir; M.T. Joghataie: mt.joghataei@yahoo.com; J. Ai: jafar_ai@tums.ac.ir; A. Pazouki: pazouki@minisergury.com; D.L. Kaplan: david.kaplan@tufts.edu; M.R. Hamblin: hamblin@helix.mgh.harvard.edu; M. Mozafari: mozafari.masoud@gmail.com; A. Samadikuchaksaraei: samadikuchaksaraei@yahoo.com

[a]Department of Tissue Engineering and Applied Cell Sciences, School of Advanced Technologies in Medicine, Tehran University of Medical Sciences (TUMS), Tehran, Iran

[b]Cellular and Molecular Research Center, Iran University of Medical Sciences (IUMS), Tehran, Iran

[c]Minimally Invasive Surgery Research Center, Iran University of Medical Sciences (IUMS), Tehran, Iran

[d]Department of Biomedical Engineering, Tufts University, 4 Colby St, Medford, MA 02155, United States

[e]Wellman Center for Photomedicine, Massachusetts General Hospital, 50 Blossom Street, Boston, MA 02114, United States

[f]Department of Dermatology, Harvard Medical School, 25 Shattuck Street, Boston, MA 02115, United States

[g]Harvard-MIT Division of Health Sciences and Technology, 77 Massachusetts Avenue, Cambridge, MA 02139, United States

[h]Bioengineering Research Group, Nanotechnology and Advanced Materials Department, Materials and Energy Research Center (MERC), Tehran, Iran

[i]Department of Tissue Engineering & Regenerative Medicine, Faculty of Advanced Technologies in Medicine, Iran University of Medical Sciences (IUMS), Tehran, Iran

[j]Department of Medical Biotechnology, Faculty of Allied Medicine, Iran University of Medical Sciences (IUMS), Tehran, Iran

Abstract

There is an unmet clinical need for novel wound healing strategies to treat full thickness skin defects, especially in diabetic patients. We hypothesized that a scaffold could perform dual roles of

*Corresponding authors at: Department of Tissue Engineering and Applied Cell Sciences, School of Advanced Technologies in Medicine, Tehran University of, Medical Sciences (TUMS), Tehran, Iran (M.T. Joghataie).

a biomechanical support and a favorable biochemical environment for stem cells. Human umbilical cord perivascular cells (HUCPVCs) have been recently reported as a type of mesenchymal stem cell that can accelerate early wound healing in skin defects. However, there are only a limited number of studies that have incorporated these cells into natural scaffolds for dermal tissue engineering. The aim of the present study was to promote angiogenesis and accelerate wound healing by using HUCPVCs and decellularized dermal matrix (DDM) in a rat model of diabetic wounds. The DDM scaffolds were prepared from harvested human skin samples and histological, ultrastructural, molecular and mechanical assessments were carried out. In comparison with the control (without any treatment) and DDM alone group, full thickness excisional wounds treated with HUCPVCs-loaded DDM scaffolds demonstrated an accelerated wound closure rate, faster re-epithelization, more granulation tissue formation and decreased collagen deposition. Furthermore, immunofluorescence analysis showed that the VEGFR-2 expression and vascular density in the HUCPVCs-loaded DDM scaffold treated group were also significantly higher than the other groups at 7 days post implantation. Since the rates of angiogenesis, re-epithelization and formation of granulation tissue are directly correlated with full thickness wound healing in patients, the proposed HUCPVCs-loaded DDM scaffolds may fulfil a role neglected by current treatment strategies. This pre-clinical proof-of-concept study warrants further clinical evaluation.

Statement of Significance—The aim of the present study was to design a novel tissue-engineered system to promote angiogenesis, re-epithelization and granulation of skin tissue using human umbilical cord perivascular stem cells and decellularized dermal matrix natural scaffolds in rat diabetic wound models. The authors of this research article have been working on stem cells and tissue engineering scaffolds for years. According to our knowledge, there is a lack of an efficient system for the treatment of skin defects using tissue engineering strategy. Since the rates of angiogenesis, re-epithelization and granulation tissue are directly correlated with full thickness wound healing, the proposed HUCPVCs-loaded DDM scaffolds perfectly fills the niche neglected by current treatment strategies. This pre-clinical study demonstrates the proof-of-concept that necessitates clinical evaluations.

Keywords

Wound healing; Decellularization; Scaffold; Stem cell; Dermal tissue engineering

1. Introduction

Chronic non-healing wounds are a major public health problem, affecting approximately 6.5 million patients in the United States [1]. Poor healing of chronic wounds is characterized by a prolonged inflammatory phase, epigenetic changes, delayed cellular proliferation, poor re-epithelialization, and impaired angiogenesis [2–4]. Angiogenesis is one of the major issues in wound healing, which is essential for the delivery of oxygen and nutrients to the cells in the wound site [5]. Diabetics in particular, suffer from poor wound healing due to impaired angiogenesis [6] and altered hyaluronan expression [7].

The use of various types of stem cells to enhance tissue and organ regeneration has recently become widely employed in the field of tissue engineering [8]. Among various types of stem cells, mesenchymal stem cells (MSCs) have been demonstrated to have beneficial functional

effects in cardiomyogenesis [9], tendon repair [10], bone regeneration [11] and dermal wound healing [12]. In addition, MSCs have been reported to contribute to wound healing by improving neovascularization and reducing scar formation, by encouraging direct differentiation, and by potent paracrine signaling that supports angiogenesis [13–15]. However, current sources of MSCs require invasive procurement procedures that provide a relatively low amount of progenitor cells. To overcome these limitations, human umbilical cord perivascular cells (HUCPVCs) have been recently reported as an alternative source of mesenchymal progenitor cells, due to their higher proliferative rate and better frequency when compared with other sources of MSCs [16,17]. Furthermore, HUCPVCs have demonstrated non-alloreactive and immunosuppressive properties that make them suitable for allogeneic applications [18]. It has been shown that human MSCs can overcome the immune system-mediated rejection normally seen in xenotransplantation protocols, and moreover can be permanently engrafted into immunocompetent rats [19]. Zebardast et al. [20] have recently shown that the delivery of HUCPVCs into wounds together with a preparation of fibrin protein, could play an important role in reconstruction of cutaneous tissues. However, it is known that one of the most challenging drawbacks and important limitations of current stem cell-based approaches is the lack of engraftment of the cells into the site of injury [21]. Therefore, incorporation of the cells into an appropriate polymeric or synthetic scaffold has shown promising results in the augmentation of cell engraftment [22]. Up to now, various biomaterials and multiple growth factors have been used to regenerate skin lesions, particularly in chronic wounds [23,24]. Considerable attention has been paid to biologic scaffolds derived from the extracellular matrix (ECM) of native tissues due to the safety and efficacy of such natural scaffolds [25,26]. The composition and ultrastructure of ECM consists of a complex combination of structural and functional proteins, glycosaminoglycans (GAGs), glycoproteins, and small molecules. Although native ECM contains only very small quantities of growth factors and cytokines, these are vital in modulating a variety of cellular activities (i.e., cell migration, proliferation, differentiation, and maturation) [27,28]. Recently, some primary studies have shown that biological scaffolds, such as decellularized dermal matrix (DDM), can significantly decrease wound area and promote healing of full thickness skin defects [29].

The objective of the present study was to determine the effects of DDM scaffolds (acting as a skin tissue-specific microenvironment) as a suitable carrier for the delivery of HUCPVCs, and to examine its therapeutic effects in an excisional wound model using diabetic rats. Moreover, after preparation and characterization of the HUCPVCs-loaded DDM scaffolds *in vitro*, they were implanted into wounds *in vivo* to understand the mechanisms that regulate wound repair in diabetic rats.

2. Materials and methods

2.1. Ethical approvals

Human umbilical cords were obtained under an IRB approved human research protocol (TUMS.REC.1395.2406) at Imam Khomeini Hospital, Tehran, Iran. Human skin samples were obtained under an IRB approved research protocol (TUMS.REC.1395.2406) at Hazrat-e Fatemeh Hospital, Tehran, Iran. Both human protocols were carried out according to the

guidelines of the Helsinki Declaration. Animal studies were carried out under an IACUC approved research protocol at Iran University of Medical Science, Tehran, Iran. Animal studies were carried out in accordance with US NIH guidelines.

2.2. Isolation and culture of HUCPVCs

The umbilical cords were obtained from consenting patients who underwent caesarian section (Imam Khomeini Hospital, Tehran, Iran) and were immediately transferred to the lab in a previously supplied vessel containing alpha minimum essential medium (α-MEM, Gibco Burlington, ON, Canada no. 12571) containing antibiotics (penicillin G at 167 units/ml; Sigma Oakville, ON, Canada no. P-3032), gentamicin (50 μg/ml; Sigma no. G-1397) and amphotericin B (0.3 μg/ml; Sigma no. A9528). The cords were dissected to 4–5 cm long pieces and blood vessels were removed after cutting the epithelium and exposing the Wharton's jelly (WJ). The ends of each dissected vessel were tied by a silk thread and placed into a Falcon tube containing a solution of 1 mg/ml collagenase (Sigma Aldrich, no. C-0130) with phosphate buffered solution (PBS). Following 4 h incubation, the suspension was collected and centrifuged. The pellets were resuspended in 10 ml PBS and counted using a hemocytometer [17]. Finally, the cells were cultured in T-75 cm^2 tissue culture polystyrene dishes in supplemented medium (SM) (75% α-MEM, 15% fetal bovine serum (FBS, Sigma Aldrich, no. F7942.CA) and 10% antibiotics, which was changed every 2 days. At passage 3, $>1 \times 10^5$ cells were treated with 2%FBS/PBS solution and diluted to 1:100 concentration. The cells were then incubated with fluorescently labeled mouse anti human antibodies including CD90-PE (Thy-1, Cat.No, FAB2067P), CD73-PE (SH3, no, 550257), CD44-FITC (no, 555478), CD105-FITC (endoglin, no, 561443), CD34-PE (no,555822), and CD45-FITC (no,555482) for 30 min at 4 °C. The primary antibody was omitted to produce negative controls (all antibodies were from, BD Bioscience, santacrose, CA).

2.3. Tissue procurement and preparation of DDM

Human skin samples were obtained and harvested from the donors, undergoing liposuction and mastectomy surgeries, (ages from 20 to 45 years) following national rules on harvesting and processing tissues at Hazrat-e Fatemeh Hospital, Tehran, Iran. The donors were screened for transmittable diseases such as the human immunodeficiency virus (HIV), hepatitis, syphilis and human T-cell lymphotropic virus (HTLV) using immunoreactive serological analysis and reverse transcription polymerase chain reaction (RT–PCR) tests. In brief, under sterile conditions split-thickness pieces of skin were removed with a dermatome and stored at −40 °C. Prior to processing, the skin samples were thawed and cut to size approximately (4×5 cm^2) and rinsed in a saline solution in supplemented with 1% antibiotic–antimycotic (Gibco Life Technologies, no. 15400062, US). The tissues were immersed in a hypotonic solution containing, 300 ml glycerol (Sigma Aldrich, no. G7757, US) l0 mM Tris buffer and 5 mM ethylenediaminetetraacetic acid (EDTA, Sigma Aldrich, no. E9884, US) on an orbital shaker, 200 RPM for 12 h at room temperature. The epidermal layers were subsequently mechanically detached from the dermis. The samples were then treated with a hypertonic solution containing 1% (w/v) triton X-100, 5 M potassium chloride (KCl), 50 mM Tris buffer with a serine protease inhibitor, phenylmethanesulfonyl fluoride, (PMSF, Sigma Aldrich, no. P7626, US) for 24 h. Then, the samples were treated with peracetic acid solution (% 0.1 v/v), on an orbital shaker, 40–45 RPM for 3 h at room

temperature. After that to entirely remove the DNA and RNA, the solution was replaced with a physiological buffer containing 1330 ml of DNAase (Sigma Aldrich, no. D4527, US) and 1330 ml of RNAase (Sigma Aldrich, no. R5125, US) for 5 h at 37 °C. Finally, the processed samples were washed several times in PBS supplemented with 1% antibiotic and antimycotic and sterilized by incubation with 0.1% peracetic acid in PBS (pH 7.2) for 3 h. The final DDM samples were stored at −196 °C. Aseptic conditions were maintained throughout all steps of the protocols. (See the decellularization process described in Supplementary Material 1)

2.4. In vitro characterization of DDM

2.4.1. Histological and ultra-structural analyses—The microstructure of the DDM scaffolds was evaluated using light microscopy and scanning electron microscopy (SEM). Prior to histological evaluation, the samples were fixed in 10% formalin for 24–48 h, and after paraffin embedding and sectioning (4–6 μm), the samples were stained with H&E and Masson's trichrome. Histological assessment was done under a light microscope (Olympus, Japan). The cellular content in the DDM was examined by staining with 6-diamidino-2-phenylindole (DAPI). For ultrastructural examination (TESCAN-VEGA TS5136MM, US), the samples were fixed with 0.25% glutaraldehyde solution and sputter-coated with gold. The samples were examined on a scanning electron microscope (TESCAN-VEGA TS5136MM, US).

2.4.2. DNA extraction—The residual DNA content in the fresh human skin and the DDM samples was determined using a commercially available kit (TIANamp Genomic DNA Kit, TIANGEN Biotech(Beijing)Co, china) and QuantiTect SYBR® Green PCR Kits, (Qiagen, Germany). The samples were freeze–dried and weighed (25–30 mg dry weight), and then the DNA extraction procedure was applied to the samples. The DNA content quantified using a NanoDrop™ spectrophotometer (thermo scientific, US) and the size of remaining DNA fragments were determined by a 2% agarose gel. Also, a Quant-iT PicroGreen assay (Invitrogen, Carlsbad, CA) was used for quantification of double-stranded DNA.

2.4.3. Tensile strength test—The mechanical properties of the fresh human skin and the DDM samples were measured using the Zwick Roell testing machine (Zwick Roell model Z0.5, Germany) equipped with a 1 kN load cell at a rate of 10 mm/min. The samples were cut into 1 × 5 cm^2 size strips, 0.5–1 mm in thickness and the gauge length of about 2 cm. The tensile parameters, maximum stress, Young's modulus and elongation at breaking point were calculated.

2.4.4. Cell viability and cytotoxicity—Cell proliferation in DDM samples was determined by 3-(4,5-dimethylthiazol-2-yl)-2,5-diphenyltetrazolium bromide (MTT) assay at different time intervals. Briefly, HUVPVCs were seeded into 24-well plates and incubated for 24 h in a 5% CO_2 at 37 °C with an initial inoculum of 20,000 cells per well. Subsequently, the uniform tissue samples were prepared from each group by using a 6 mm biopsy punch, weighed and placed in a 24-well plate. Then, after preparation of a 10 ml MTT solution (5 mg/ml; Sigma Aldrich, USA), 100 μl (0.5 mg/ml in PBS) was added into each well, and the cells were incubated for 4 h at 37 °C. Next, the medium was decanted and

600 μl dimethyl sulfoxide (DMSO, Sigma Aldrich, no. D8418, US) was added for 15 min. The optical density (OD) values were read on a spectrophotometer at 570 nm wavelength.

2.5. Recellularization of DDM with HUCPVCs

The DDM samples were washed in PBS and cut into 20 mm pieces. The HUCPVCs were seeded onto the DDM scaffolds at a density of 1×10^6 cells/cm^2 in Dulbecco's modified Eagle's medium (DMEM, Gibco, Thermo Fisher Science, no. 10567–014, US) supplemented with 10% (w/v) fetal bovine serum (Sigma Aldrich, no. F7942.CA), 80 $\mu g.L^{-1}$ gentamycin(Sigma Aldrich, no. G1397, US). The HUCPVCs-loaded DDM scaffolds were incubated at 37 °C and %5 CO_2. The morphology and attachment of the cells on the surfaces of DDM scaffolds were observed by SEM (TESCAN-VEGA TS5136MM, US).

2.6. In vivo assessment on diabetic rat models

2.6.1. The streptozotocin-induced diabetic rat models—Adult male wistar rats, with average body weight 200–250 g, were provided from the Animal Laboratory in Iran University of Medical Science (IUMS), Tehran, Iran. For this purpose, rats (n = 54) were rendered diabetic by using a single dose (75 mg/kg) intraperitoneal injection of streptozotocin (STZ; Sigma Aldrich, US) in 0.1 M citrate buffer (pH = 4)(enzyme grade; Fisher). The blood glucose level was measured using an electronic device (Glucometer, Accu-Check, Germany) at days 0, 3 and 7. Animals showing a blood glucose concentration >15 mM, together with weight loss, polyuria and polydipsia were considered as diabetic. One week later, the animals were prepared for the wound-healing test. The rats were anaesthetized with intraperitoneal injection of ketamine (50 mg/kg) and xylazine (15 mg/kg) before surgery, the dorsal surface of the animal was shaved with an electric clipper and cleaned with 5% povidone-iodine solution. A circular excisional, full-thickness cutaneous wound, with a diameter of 20 mm was created on the back of each rat, and then grafted with different scaffolds. A 20 × 20 mm-sized scaffold was implanted and sutured into wound site using 3-0 synthetic absorbable sutures (PGA suture). The sutures disappeared over 7 days and the grafts were subsequently integrated into the host tissue. The diabetic rats were randomly divided into three group: the control (blank group), receiving DDM (scaffold without cells) and receiving HUCPVCs-loaded DDM scaffolds.

2.6.2. Wound healing assay and histological examination—The rats were sacrificed using CO_2 gas asphyxiation according to AVMA guidelines for the euthanasia of animals [30]. The tissue samples (two samples from each rat) were collected by excising the graft together with a surrounding rim of normal skin at days 7, 14 and 21, fixed in 4% paraformaldehyde, dehydrated in ethanol, cleared in xylene and embedded in paraffin. The samples were sectioned at 6 μm and stained with H&E and Masson's trichrome for histological examination. Collagen deposition, wound re-epithelization, granulation tissue formation and inflammatory cells were analyzed after 7 days in each group. Wound closure was defined as percentage closure of the wound bed, measured at days 7, 14 and 21 by using image J software (Image J version 1.4). To this end, high resolution images were captured from the each specimen at 10× magnification. The percentage of wound closure was calculated according to:

$$\% \text{ wound closure} = (A_0 - A_t) / A_0 \times 100$$

A_0 = Area of original wound

A_t = Area of actual wound

Wound maturity was investigated using the wound cellular profile at 7 days after surgery according to the following scoring system [31]. Score 1: limited cells present or highly inflammatory cells; Score 2: predominantly inflammatory cells; Score 3: equivalence between inflammatory and proliferative cells; Score 4: predominantly proliferative cells; Score 5: highly proliferative cells. In addition, the percentage of collagen deposition was measured by Masson trichrome staining. An optical microscope was used to capture micrographs from the sections. IPP 6.0 software was used for analysis by two independent researchers [32].

2.7. Angiogenesis determination

Fluorescent immunostaining for endothelial cell markers (VEGFR2) was done in wound samples from each group, taken at day 7, to detect whether angiogenesis had occurred in the granulation tissues of the wound bed. The paraffin embedded tissue sections were incubated with rabbit polyclonal primary antibody to VEGF receptor 2 (1:100, Abcam, USA) at 4 °C overnight and then the sections were incubated with goat *anti*-rabbit IgG H&L secondary antibody (1:50, Abcam, USA) for 90 min at room temperature. DAPI dye (Sigma Aldrich, no. D9542, US) was used to stain the nuclei. Capillary density was determined by counting the vascular structures positively stained with VEGFR2 in three random fields/section.

2.8. Statistical analysis

All experiments were performed six times. The outcomes including cell viability, wound closure percentage, length of newly formed epithelium and collagen deposition percentage compared between three groups and times with repeated measure ANOVA. In addition, one-way ANOVA with Bonferroni post-hoc was used for the analysis of epithelization thickness, granulation tissue thickness, capillary density and wound maturity. All data presented as the mean ± standard error of mean. Statistical analysis was performed using (SPSS 18.0 software, Chicago, IL, USA).

3. Results

3.1. Morphology and flow cytometry analysis

The adherent cultured HUPVCs showed a spindle-shaped morphology when observed using a phase-contrast microscope (Supplementary Material 2). Flow cytometry analysis was used to confirm that the extracted cells were human umbilical cord perivascular cells. This test showed that purity of the cell surface markers CD90, CD73, CD44 and CD105 populations was 93.83%, 84.91%, 84.08% and 73.43%, respectively. Whereas the CD34-positive, CD45-positive population were only 0.57% and 1.03%, respectively (Supplementary 3).

3.2. Characterization of the DDM

3.2.1. Histological and DNA content evaluations—The processed tissue was assessed microscopically after H&E and Masson's trichrome staining. The results showed that all the cellular content had been removed from the dermis after the decellularization process without any deterioration of its structural integrity. In addition, to assure the efficient removal of cellular nuclei after processing, the dermal tissues were stained before and after decellularization with DAPI (4′, 6-diamidino-2-phenylindole), in which the DDM sample showed no cellular nuclei using fluorescence microscopy. Fig. 1 shows that the decellularization process accomplished complete removal of epidermis layer and its appendages including hair ducts and sweat glands.

The DNA quantification in the DDM scaffolds show that no DNA ⩾200 base pairs was observed by agarose gel analysis (Fig. 2A and Table 1). Furthermore, the Quant-iT PicroGreen analysis for residual DNA content, demonstrated that the dermis before the decellularization process had a dsDNA content of 348.86 ng/mg, and that this was reduced to 30.59 ng/mg (>90% removed) after the decellularization process ($P < 0.001$) (see Fig. 2B).

3.2.2. Cell viability and cytotoxicity evaluations—The results showed that there was no significant difference between the different samples. Fig. 3A shows the SEM micrographs of the interaction of the DDM scaffolds in contact with the HUCPVCs, indicating that the cells were attached and evenly distributed on the surface of the scaffold. The extended lamellipodia of HUCPVCs were observed in the DDM scaffolds. As shown in Fig. 3B, cell proliferation was better in both tissue samples at all time points compared with cell proliferation found in tissue culture plates (TCP). However, the best result was found in the DDM group at days 5 and 7 with a slight increase in the number of cells compared with the fresh dermis sample. To make sure that the cells could survive and migrate within the DDM scaffolds, HUCPVCs loaded–DDM scaffolds were evaluated histologically after 7 days *in vitro* culture, as shown in Fig. 3C, the histologic staining, indicated that a large number of cells were distributed throughout the cross-section of the DDM scaffold, Although the seeded cells had primarily expanded on the surface of the scaffolds, numerous cells were also identified in deeper parts of the scaffold (see Fig. 4).

3.2.3. Biomechanical behavior—To ensure that the processing of DDM did not affect its structural integrity, a tensile strength test was conducted. The extracted results from the stress-strain curves are shown in Table 2. It is found that the fresh dermis tissue could be decellularized without any deterioration in its biomechanical properties. Although the decellularized dermis appeared to be visually thinner and weaker than human fresh dermis, there were no statistically significant differences between these samples in terms of maximum load, tensile strength and Young's modulus. It is a favorable feature of the process that during the decellularization of the dermis, no additional cross-linkers were used (such as glutaraldehyde) that may show cytotoxicity. Some studies have reported lower mechanical properties of DDM [33–35], and investigators have made attempts to develop further strategies for the improvement of the mechanical properties [36,37]. The same results were

also obtained for the suture retention strength test, indicating that there was no meaningful difference between both samples.

3.3. Wound healing effect of the scaffolds on diabetic rat wounds

We sought to assess the role of the scaffolds in healing of full thickness excisional diabetic wounds, to better observe the effect of HUCPVCs on the healing process. As can be seen in Fig. 5, the rat wounds implanted with HUCPVCs-loaded DDM scaffolds exhibited an accelerated wound closure at day 14 and 21 as compared with the rats treated with DDM alone and the untreated control wounds. The obtained results also showed that the wound closure process was significantly faster for the HUCPVCs-loaded DDM scaffolds with a mean wound closure of 42.04 ± 2.02%, compared to the control group with a mean closure of 21.41 ± 2.98% at day 7 ($P < 0.001$). Furthermore, there was no significant difference between the HUCPVCs-loaded and unloaded DDM scaffolds at 7 days. In the rat wounds receiving implantation of the HUCPVCs-loaded DDM scaffolds, the wound closure rate was 86.12 ± 2.52% and 96.4 ± 3.2% at 14 and 21 days, respectively, whereas for the control group the wound closure rate at days 14 and 21, was 29.50 ± 2.38% and 55.38 ± 31.19% ($P < 0.001$), respectively. However, there was a significant difference between the HUCPVCs-loaded and unloaded DDM scaffolds at 14 and 21 days. The wound closure rate for the unloaded DDM scaffolds was 59.21 ± 5.26% and 79.95 ± 2.19 at 14 and 21 days ($P < 0.001$ vs HUPVCs-loaded) (see Fig. 5).

The histological analysis of the implanted scaffolds, using H&E staining, are presented in Fig. 6. As can be seen a high number of fibroblasts and inflammatory cells with infiltration into the upper layers of dermis were clearly observable in the wound site in the control group at 7 days post-surgery. The result showed that irregular collagen fibers and granulation tissue was formed during this time point for the HUCPVCs-loaded and -unloaded DDM scaffolds. The moderate inflammation remained in the control group until 14 days, as shown by presence of inflammatory cells. Also, the epidermal layer was completely formed in the HUCPVCs loaded-DDM treated group and this fully covered the wound site at 14 days post implantation, while in control and DDM treated wounds the re-epithelialization was not fully completed. Overall the HUCPVCs loaded-DDM group showed a higher efficacy of wound healing in comparison with the control and DDM groups.

Moreover, to further assess the effect of the HUCPVCs-loaded DDM scaffolds on wound healing, the thickness of the granulation tissue and extent of re-epithelialization were both analyzed by microscopic evaluation. The results indicated that the thickness of granulation tissue in the HUCPVCs-loaded DDM group was significantly higher than that of the DDM and control groups at day 7 post-implantation *in vivo* ($P < 0.001$), as shown in Fig. 7A. However, no significant differences were found between the control and DDM groups. Indeed, the HUCPVCs-loaded DDM scaffolds-treated wounds demonstrated an increased thickness in the newly regenerated epidermis at 7 days compared with the other groups. The epidermal layer thickness in the HUCPVCs-loaded DDM group was 67.76 ± 19.34 μm, while this data for the DDM and control groups were 55.00 ± 8.48 μm and 30.55 ± 12.08 μm, respectively (see Fig. 7B).

Furthermore, the result of the wound maturity score are shown in Fig. 7C, in which the maturity score in HUCPVCs-loaded DDM treated group in the central part of the wound was significantly different from the other groups at 7 days ($P < 0.001$, Mann–Whitney U-test, Fig. 7c), while no significant differences in wound maturity were observed in the marginal parts of the treated wounds. When the impact of treatments on the experimental groups was considered, wound maturity was significantly promoted in the central wound areas of the HUCPVCs-DDM group (3.57 ± 1.16) compared to DDM alone (2.76 ± 0.6) and control groups (2.32 ± 1.07), respectively.

Masson's trichrome images showed that newly formed collagen bundles could be identified in DDM and HUCPVCs-loaded DDM treated groups compared with the control group after 14 days (see Fig. 8). Subsequently, additional collagen accumulation and deposition was observed in the control group at 21 days post-surgery. The basket-weave pattern typical of collagen fibers was observed for the HUCPVCs-loaded DDM treated group at 21 days. In contrast, the collagen fiber bundles were arranged in a parallel form in the other 2 groups. In addition, a lack of specific organization of collagen fibers and the presence of a visible scar was identified in the DDM and control groups at the same time point. It is worth mentioning that vascular structures, nerves and skin appendages were also detectable in the HUCPVCs-loaded DDM treated group at 21 days post implantation. Furthermore, collagen deposition in the wounds treated with HUCPVCs-loaded DDM scaffolds was relatively similar to that found in normal skin, showing that dermal regeneration was enhanced by the use of HUCPVCs-loaded DDM scaffolds.

The results of the HUCPVCs-loaded and unloaded DDM scaffolds on the re-epithelization process showed that the length of the newly regenerated epidermal layer and its thickness were significantly higher for the HUCPVCs-loaded DDM scaffolds presumably due to the presence of the HUCPVCs at their site of action. As can be seen, re-epithelization was enhanced in the DDM treated wounds after 14 days. In addition, complete re-epithelization was observed in HUCPVCs-loaded DDM groups. There was no significant difference between the length of newly regenerated epidermis in the DDM and control groups at 7 days. The re-epithelization rate of difference groups is shown in Fig. 9A. As can be seen, the length of the newly regenerated epidermis in HUCPVCs-loaded DDM treated group at 7 and 14 days were 744 ± 71.3 μm and 1195.04 ± 32.90 μm, respectively, indicating that these values were higher than that of control group with the length mean of 362.80 ± 15.62 μm and 836.80 ± 13.43 μm in the same time points ($P < 0.001$). In addition, the length of the newly regenerated epidermis for the DDM treated group were 366.06 ± 32.69 μm and 956.15 ± 12.52 μm at 7 and 14 days, respectively.

The effect of implantation of HUCPVCs-loaded DDM scaffolds on the percentage of collagen deposition was analyzed by Masson's trichrome staining of the wound tissues 21 days after implantation and then compared with the other groups. It was found that the collagen deposition percentages for control group, DDM and HUCPVCs-loaded DDM treated groups were 96.4 ± 2.72%, 82.2 ± 2.88% and 70 ± 3.4% at 21 days post-surgery, respectively ($P < 0.001$), indicating that collagen deposition in the control group was significantly higher than the other groups. However, no significant difference was observed between different groups at 14 days (see Fig. 9B).

3.4. Angiogenesis activity of the scaffolds in the diabetic rat model

The pro-angiogenic effect of HUCPVCs-loaded DDM scaffolds on diabetic rat wounds was determined by histological and immunohistochemical analysis. As shown in Fig. 10, the neovascularization increased in the HUCPVCs-loaded DDM treated group compared with the other groups at 7 days and 14 days. Surprisingly, large number of mature vessels were clearly observed in HUCPVCs-loaded DDM treated groups as early as 7 days. Furthermore, immunohistochemical analysis of wound tissue was performed to detect VEGFR-2 expression in the excised tissues. As shown in Fig. 11, the capillary density in HUCPVCs-loaded DDM treated groups was higher than those of control and DDM groups after 7 days of implantation. Quantitatively, the HUCPVCs-loaded DDM treated group had a higher value of capillary density compared with the other groups. The results suggested that the amount of VEGF-R2 expression, which has an important role in angiogenesis and wound healing, increased in the HUCPVCs-loaded DDM treated group, and subsequently promoted angiogenesis in the wound (Fig. 11).

4. Discussion

It is known that the efficiency of the wound healing process in both chronic and non-chronic wounds is affected by a number of factors such as a sufficient blood supply, an appropriately timed inflammation process, and sufficient expression of essential growth factors in the wound area [38,39]. Therefore, there have recently been attempts among tissue engineers and biologists to design effective tissue implants, and interventions that could accelerate the wound healing process. Since wound closure is notably impaired in diabetic patients, stem cell transplantation could significantly enhance the healing process, promoting pro-angiogenesis activity, stimulating cell proliferation and migration, and improving granulation tissue and re-epithelization [40]. On the other hand, full thickness skin wounds cannot be perfectly healed with no residual scarring, without using a dermal substitute [41]. Therefore, this study aimed to develop a dermal substitute that could function to effectively deliver stem cells to the wound bed. The present study was designed to determine the effect of HUCPVCs on the angiogenesis activity and regeneration of full-thickness skin defect in diabetic rat wounds. The isolated MSCs from the perivascular tissue of the human umbilical cord are immunocompatible and multipotent with a high rate of proliferation, which makes them excellent candidates for the acceleration of the wound healing process [18,42].

The current therapies for diabetic wounds include debridement, negative pressure therapy, control of infection and normalization of glycemic levels. Moreover, regenerative medicine approaches including the use of growth factors, cells and gene therapy, cannot completely resolve the healing problem. All the these methods suffer from some drawbacks. For instance, the short half-life, and some toxicity after administration are limitations of growth factor therapy [43] Adipose derived stem cells (ASCs) and bone marrow derived stem cells (BMSCs) are common sources for cell therapy, but a variety of invasive methods are required for harvesting them [44]. The presently described HUCPVCs-loaded DDM scaffold is a cellular dermal substitute consisting of a scaffold with a structure and composition similar to that found in natural human dermis, and which also possesses adequate mechanical properties. In addition, the HUCPVCs are multipotent cells that can be isolated

completely non-invasively from discarded human umbilical cords. Although it might be a little challenging to obtain a sufficient amount of HUCPVCs, the suggested non-invasive method for the isolation of this class of cells could make it a better candidate for many different kinds of tissue engineering applications.

To establish a delivery system for the cells, a previously developed protocol [45] was modified for the decellularization of human dermis. As shown in Fig. 1, all detectable cellular elements were completely removed from the treated human dermis after the decellularization process. Histological examination also confirmed that the structure of DDM and its biomechanical strength were relatively similar to those of fresh human dermis. This protocol has been shown to have superior advantages over conventional protocols due to the use of glycerol which preserves the fundamental structure of the dermis and its mechanical properties. DDM has remarkable antiviral properties, appropriate antigenicity and immunocompatibility, and has the advantage of the ease of epidermis removal [46,47]. Peracetic acid was also used because of its ability to eradicate nucleic acids from the treated tissues, and for its antiseptic properties [48,49].

The presence of any residual DNA content in decellularized tissues is always a major obstacle to its function as a scaffold for tissue regeneration. Therefore, PCR and PicroGreen analyses were used to confirm that the entire structure of the dermis was cleared from any DNA content after treatment [50]. After seeding the HUCPVCs into the DDM scaffolds, SEM and histology analysis showed that the cells were successfully attached to the scaffold walls after 5 days of *in vitro* culture. This is in agreement with data from Bondioli et al. [27] who suggested that porous three-dimensional structures having biological ligands on their surfaces can significantly promote attachment, proliferation, migration and differentiation of the seeded cells. The ECM-like ultrastructure of the DDM scaffolds could provide the required ligands for cell attachment that facilitate the cellular communications between the adjacent cells. Moreover, some components of the DDM scaffolds (glycosaminoglycans and proteoglycans) can bind to growth factors and cytokines [51]. Therefore, the prepared DDM scaffold is expected to not only act as a useful material for tissue engineering but could also positively regulate some aspects of cellular behavior.

The data showed that the HUCPVCs-loaded DDM scaffolds enhanced healing of full thickness excisional wounds in diabetic rats by affecting granulation tissue formation, epithelial regeneration, and pro-angiogenesis activity via expression of VEGFR-2, all of which will help to improve the wound closure rate. In a recent study, Zabadast et al. [20]. reported that HUCPVCs-seeded into fibrin constructs produced a high rate of re-epithelization and improved wound strength without any sign of wound contraction. It is known that there are some differences in the wound healing process in rodent and human skin. The main reason of wound contraction that normally happens in rodent skin is basically due to the existence of a layer situated directly below the skin (paniculosus carnosus layer), while the healing in humans only occurs via re-epithelization and granulation tissue formation [52]. Therefore, in our study, the wound model was created by harvesting full-thickness skin and superficial fascia, in order to prevent wound contraction. The presence of HUCPVCs is likely to have enhanced the healing rate of the wound by accelerating granulation tissue formation and epithelial regeneration. It can be also

suggested that better wound regeneration occurred due to some secretory activity of the HUCPVCs [20,53], and the use of the DDM scaffold which promoted retention of the cells at the wound site. Some previous studies have also reported on the contribution of different stem cells in the wound healing process by affecting both migration and proliferation of fibroblasts and keratinocytes which play essential roles in extra cellular matrix formation [54].

Masson's trichrome staining showed that the percentage of collagen deposition significantly increased in the control and DDM treated groups at 21 days post-surgery. Since collagen deposition is a measure of scar formation [55], it can be suggested that HUCPVCs could reduce scar formation in diabetic wounds possibly due to shortening of the inflammatory phase and improved remodeling at the wound site. The present findings are also in agreement with research conducted by Fathke et al. [56] who identified stem cells as major contributing factors for the reduction of collagen deposition. They showed that bone marrow mesenchymal stem cells (BMCs) could produce both collagen type I and collagen type II during the healing process, while only collagen type I was reported to be produced by the resident skin cells.

It has been reported that diabetic patients suffer from impaired angiogenesis [57]. Many studies have confirmed that well-functioning angiogenesis and a sufficient blood supply are two important factors that directly affect the wound healing process [58,59]. The obtained results from the diabetic rat wounds treated with the DDM scaffolds seeded with HUCPVCs at days 7 and 14 post implantation showed an enhancement in angiogenesis activity when compared with the other groups. It is known that neovascularization is essential to preserve the newly organized tissue [60]. Also a strong relationship between angiogenesis and VEGR-2 expression has been reported in the literature [59,61]. We hypothesized that elevated levels of VEGFR-2 expression in the HUCPVCs-loaded DDM treated groups might be due to the paracrine effects of HUCPVCs in stimulating angiogenesis.

To have a better understanding of angiogenesis activity, the capillary density was measured by counting the number of blood vessels. The results showed that capillary density was significantly higher in the HUCPVCs-loaded DDM scaffolds treated groups when compared with the other groups. Previous studies have reported that some angiogenic factors such as VEGF, bFGF, TGFβ1 and angiopoetin-1 could be released by HUCPVCs after transplantation, and could accelerate the angiogenesis and vasculogenesis activities [62]. For example, bFGF can bind to heparan sulfate proteoglycan in the ECM, and mediate mitogenesis and angiogenesis [63]. Furthermore, endothelial cell migration is stimulated by low oxygen tension [64]. It has been frequently reported that chronic wounds are always in a hypoxic condition. This microenvironment affects expression of pluripotency markers such as OCT4, SOX2 and Nanog in the seeded HUCPVCs, which can improve the clonogenicity potential in the cells [65]. The released VEGF-A from HUCPVCs can bind to the VEGF receptor-2 located on the endothelial surface of blood vessels. This interaction between ligand and receptor is critical for angiogenesis activity in wound sites [66]. The pro-angiogenesis capacity of stem cells seeded on an engineered biomimetic hydrogel scaffold was recently assessed in detail by Rustad et al. [67]. They suggested that their scaffolds

could supply a functional environment for proliferation of stem cells that increase the level of pro-angiogenic cytokines.

It can be supposed that the engraftment and survival of HUCPVCs is enhanced when they interact with the DDM scaffolds. This enhancement can be shown by improved proliferation, differentiation, expression of VEGFR-2 pro-angiogenic factor and many other cytokines. Taken together, the findings confirm that the HUCPVCs-loaded DDM scaffolds exerted beneficial therapeutic effects on diabetic wounds by enhancing angiogenesis activity and improving the overall wound healing process.

5. Conclusion

This study has successfully demonstrated the importance of HUCPVCs-loaded DDM scaffolds in enhancing cutaneous wound healing in diabetic rat wounds. The DDM scaffolds were shown to be appropriate systems for the delivery of HUCPVCs and engraftment of the cells into the wound site which is very important for controlling their fate and enhancing therapeutic efficacy. In addition, the data indicated that wound closure, re-epithelization and granulation tissue formation were enhanced for the rat wounds implanted with HUCPVCs-loaded DDM scaffolds. The most significant finding to emerge from this study was that percentage of collagen deposition in the HUCPVCs-loaded DDM treated group was significantly lower than the other groups at the same time points, suggesting that scarring might be controlled. This study is the first to suggest a significant role for HUCPVCs-loaded DDM scaffolds in promoting the wound healing process and angiogenesis via a paracrine mechanism. This effective strategy demonstrates potential advantages of HUCPVCs in angiogenesis, re-epithelization and granulation tissue which are all essential for dermal tissue engineering.

Supplementary Material

Refer to Web version on PubMed Central for supplementary material.

Acknowledgments

This work was financially supported by Iran National Science Foundation (INSF) through research Grant No. 92031133. Michael R Hamblin was supported by US NIH grant R01AI050875.

Appendix A. Supplementary data

Supplementary data associated with this article can be found, in the online version, at http://dx.doi.org/10.1016/j.actbio.2016.08.053.

References

1. McDaniel JC, Browning KK. Smoking, chronic wound healing, and implications for evidence-based practice. J Wound Ostomy Cont Nurs. 2014; 41(5):415–423.
2. Martin P. Wound healing-aiming for perfect skin regeneration. Science. 1997; 276:75–81. [PubMed: 9082989]
3. Gough NR. Reconstituting angiogenesis in vitro. Sci Signal. 2013; 6:273.

4. Gainza G, Pastor M, Aguirre JJ, Villullas S, Pedraz JL, Hernandez RM, Igartua M. A novel strategy for the treatment of chronic wounds based on the topical administration of rhEGF-loaded lipid nanoparticles: in vitro bioactivity and in vivo effectiveness in healing-impaired db/db mice. J Control Release. 2014; 185:51–61. [PubMed: 24794895]
5. Bremer AA. MnSOD, angiogenesis, and wounds: let the healing begin. Sci Transl Med. 2010; 2(59): 59–181.
6. Francis-Goforth KN, Harken AH, Saba JD. Normalization of diabetic wound healing. Surgery. 2010; 147(3):446–449. [PubMed: 19703697]
7. Shakya S, Wang Y, Mack JA, Maytin EV. Hyperglycemia-induced changes in hyaluronan contribute to impaired skin wound healing in diabetes: review and perspective. Int J Cell Biol. 2015; 2015:11.
8. Liu Y, Wang L, Kikuiri T, Akiyama K, Chen C, Xu X. Mesenchymal stem cell–based tissue regeneration is governed by recipient T lymphocytes via IFN-γ and TNF-α. Nat Med. 2011; 17:1594–1602. [PubMed: 22101767]
9. Behfar A, Crespo-Diaz R, Terzic A, Gersh BJ. Cell therapy for cardiac repair–lessons from clinical trials. Nat Rev Cardiol. 2014; 11(4):232–246. [PubMed: 24594893]
10. Moshaverinia A, Xu X, Chen C, Ansari S, Zadeh HH, Snead ML, Shi S. Application of stem cells derived from the periodontal ligament or gingival tissue sources for tendon tissue regeneration. Biomaterials. 2014; 35(9):2642–2650. [PubMed: 24397989]
11. Zeitouni S, Krause U, Clough BH, Halderman H, Falster A, Blalock DT, Chaput CD, Sampson HW, Gregory CA. Human mesenchymal stem cell-derived matrices for enhanced osteoregeneration. Sci Transl Med. 2012; 4(132):132–155.
12. Branski LK, Gauglitz GG, Herndon DN, Jeschke MG. A review of gene and stem cell therapy in cutaneous wound healing. Burns. 2009; 35(2):171–180. [PubMed: 18603379]
13. Bhang SH, Lee S, Shin JY, Lee TJ, Jang HK, Kim BS. Efficacious and clinically relevant conditioned medium of human adipose-derived stem cells for therapeutic angiogenesis. Mol Ther. 2014; 22(4):862–872. [PubMed: 24413377]
14. Hemphill C, Stavoe K, Khalpey Z. First in man: amniotic stem cell injection promotes scar remodeling and healing processes in late-stage fibrosis. Int J Cardiol. 2014; 174(2):442–443. [PubMed: 24768371]
15. Stappenbeck TS, Miyoshi H. The role of stromal stem cells in tissue regeneration and wound repair. Science. 2009; 324(5935):1666–1669. [PubMed: 19556498]
16. Capelli C, Gotti E, Morigi M, Rota C, Weng L, Dazzi F. Minimally manipulated whole human umbilical cord is a rich source of clinical-grade human mesenchymal stromal cells expanded in human platelet lysate. Cytotherapy. 2011; 13:786–801. [PubMed: 21417678]
17. Sarugaser R, Ennis J, Stanford WL, Davies JE. Isolation, propagation, and characterization of human umbilical cord perivascular cells (HUCPVCs). Methods Mol Biol. 2009; 482:269–279. [PubMed: 19089362]
18. Ennis J, Gotherstrom C, Le Blanc K, Davies JE. In vitro immunologic properties of human umbilical cord perivascular cells. Cytotherapy. 2008; 10(2):174–181. [PubMed: 18368596]
19. Grinnemo KH, Mansson A, Dellgren G, Klingberg D, Wardell E, Drvota V, Tammik C, Holgersson J, Ringden O, Sylven C, Le Blanc K. Xenoreactivity and engraftment of human mesenchymal stem cells transplanted into infarcted rat myocardium. J Thorac Cardiovasc Surg. 2004; 127(5): 1293–1300. [PubMed: 15115985]
20. Zebardast N, Lickorish D, Davies JE. Human umbilical cord perivascular cells (HUCPVC): a mesenchymal cell source for dermal wound healing. Organogenesis. 2010; 6(4):197–203. [PubMed: 21220956]
21. Chen FM, Wu LA, Zhang M, Zhang R, Sun HH. Homing of endogenous stem/progenitor cells for in situ tissue regeneration: promises, strategies, and translational perspectives. Biomaterials. 2011; 32(12):3189–3209. [PubMed: 21300401]
22. Geesala R, Bar N, Dhoke NR, Basak P, Das A. Porous polymer scaffold for on-site delivery of stem cells–protects from oxidative stress and potentiates wound tissue repair. Biomaterials. 2016; 77:1–13. [PubMed: 26576045]

23. Akar B, Jiang B, Somo SI, Appel AA, Larson JC, Tichauer KM, Brey EM. Biomaterials with persistent growth factor gradients in vivo accelerate vascularized tissue formation. Biomaterials. 2015; 72:61–73. [PubMed: 26344364]
24. Zhao S, Li L, Wang H, Zhang Y, Cheng X, Zhou N, Rahaman MN, Liu Z, Huang W, Zhang C. Wound dressings composed of copper-doped borate bioactive glass microfibers stimulate angiogenesis and heal full-thickness skin defects in a rodent model. Biomaterials. 2015; 53:379–391. [PubMed: 25890736]
25. Gholipourmalekabadi M, Bandehpour M, Mozafari M, Hashemi A, Ghanbarian H, Sameni M. Decellularized human amniotic membrane: more is needed for an efficient dressing for protection of burns against antibiotic-resistant bacteria isolated from burn patients. Burns. 2015; 41:1488–1497. [PubMed: 26048133]
26. Sonia Z, Mozafari M, Natasha G, Tan A, Cui Z, Seifalian AM. Hearts beating through decellularized scaffolds: whole-organ engineering for cardiac regeneration and transplantation. Crit Rev Biotechnol. 2015:1–11.
27. Bondioli E, Fini M, Veronesi F, Giavaresi G, Tschon M, Cenacchi G, Cerasoli S, Giardino R, Melandri D. Development and evaluation of a decellularized membrane from human dermis. J Tissue Eng Regen Med. 2014; 8(4):325–336. [PubMed: 22689414]
28. Kim SH, Turnbull J, Guimond S. Extracellular matrix and cell signalling: the dynamic cooperation of integrin, proteoglycan and growth factor receptor. J Endocrinol. 2011; 209(2):139–151. [PubMed: 21307119]
29. Li X, Meng X, Wang X, Li Y, Li W, Lv X, Xu X, Lei Z, Li J. Human acellular dermal matrix allograft: a randomized, controlled human trial for the long-term evaluation of patients with extensive burns. Burns. 2015; 41(4):689–699. [PubMed: 25687834]
30. Leary S, Underwood W, Anthony R, Cartner S, Corey D, Grandin T, Greenacre C, Gwaltney-Brant S, McCrackin MA, Meyer R, Miller D, Shearer J, Yanong R. AVMA guidelines for the euthanasia of animals. 2013:102.
31. Hardwicke JT, Hart J, Bell A, Duncan R, Thomas DW, Moseley R. The effect of dextrin-rhEGF on the healing of full-thickness, excisional wounds in the (db/db) diabetic mouse. J Control Release. 2011; 152(3):411–417. [PubMed: 21435363]
32. Wang Y, Xu R, Luo G, Lei Q, Shu Q, Yao Z, Li H, Zhou J, Tan J, Yang S, Zhan R, He W, Wu J. Biomimetic fibroblast-loaded artificial dermis with “sandwich” structure and designed gradient pore sizes promotes wound healing by favoring granulation tissue formation and wound re-epithelialization. Acta Biomater. 2016; 30:246–257. [PubMed: 26602823]
33. Healy CM, Boorman JG. Comparison of E-Z Derm and Jelonet dressings for partial skin thickness burns. Burns Incl Therm Inj. 1989; 15(1):52–54. [PubMed: 2720457]
34. MacLeod TM, Cambrey A, Williams G, Sanders R, Green CJ. Evaluation of Permacol as a cultured skin equivalent. Burns. 2008; 34(1):169–175.
35. Vitacolonna M, Mularczyk M, Herrle F, Schulze TJ, Haupt H, Oechsner M, Pilz LR, Hohenberger P, Rossner ED. Effect on the tensile strength of human acellular dermis (Epiflex(R)) of in-vitro incubation simulating an open abdomen setting. BMC Surg. 2014; 14:7. [PubMed: 24468201]
36. Gholipourmalekabadi M, Mozafari M, Salehi M, Seifalian A, Bandehpour M, Ghanbarian H, Urbanska AM, Sameni M, Samadikuchaksaraei A, Seifalian AM. Development of a cost-effective and simple protocol for decellularization and preservation of human amniotic membrane as a soft tissue replacement and delivery system for bone marrow stromal cells, Adv. Health Mater. 2015; 4(6):918–926.
37. Hogg P, Rooney P, Ingham E, Kearney JN. Development of a decellularised dermis. Cell Tissue Bank. 2013; 14(3):465–474. [PubMed: 22875198]
38. Guo S, Dipietro LA. Factors affecting wound healing. J Dent Res. 2010; 89(3):219–229. [PubMed: 20139336]
39. Kolluru GK, Bir SC, Kevil CG. Endothelial dysfunction and diabetes: effects on angiogenesis, vascular remodeling, and wound healing. Int J Vasc Med. 2012; 2012:918267. [PubMed: 22611498]
40. Wu Y, Chen L, Scott PG, Tredget EE. Mesenchymal stem cells enhance wound healing through differentiation and angiogenesis. Stem Cells. 2007; 25(10):2648–2659. [PubMed: 17615264]

41. Guo R, Teng J, Xu S, Ma L, Huang A, Gao C. Comparison studies of the in vivo treatment of full-thickness excisional wounds and burns by an artificial bilayer dermal equivalent and J-1 acellular dermal matrix. Wound Repair Regen. 2014; 22(3):390–398. [PubMed: 24844338]
42. Emrani H, Davies JE. Umbilical cord perivascular cells: a mesenchymal cell source for treatment of tendon injuries. Open Tissue Eng Regen Med J. 2011; 4:112–119.
43. Pradhan L, Andersen ND, Nabzdyk C, LoGerfo FW, Veves A. Wound-healing abnormalities in diabetes and new therapeutic interventions. US Endocrinol. 2007; 1:68–72.
44. Wong VW, Gurtner GC. Tissue engineering for the management of chronic wounds: current concepts and future perspectives. Exp Dermatol. 2012; 21(10):729–734. [PubMed: 22742728]
45. Gratzer. Methods for tissue decellularization. United States patent application publication. 2013; 38
46. Hoekstra MJ, Kreis RW, du Pont JS. History of the Euro Skin Bank: the innovation of preservation technologies. Burns. 1994; 20(Suppl 1):S43–S47. [PubMed: 8198743]
47. Richters CD, Hoekstra MJ, van Baare J, du Pont JS, Kamperdijk EW. Morphology of glycerol-preserved human cadaver skin. Burns. 1996; 22(2):113–116. [PubMed: 8634116]
48. Baldry MG. The bactericidal, fungicidal and sporicidal properties of hydrogen peroxide and peracetic acid. J Appl Bacteriol. 1983; 54(3):417–423. [PubMed: 6409877]
49. Hrebikova H, Diaz D, Mokry J. Chemical decellularization: a promising approach for preparation of extracellular matrix. Biomed Pap Med Fac Univ Palacky Olomouc Czech Repub. 2015; 159(1): 12–17. [PubMed: 24145768]
50. Gilbert TW, Freund JM, Badylak SF. Quantification of DNA in biologic scaffold materials. J Surg Res. 2009; 152(1):135–139. [PubMed: 18619621]
51. Eming SA, Hubbell JA. Extracellular matrix in angiogenesis: dynamic structures with translational potential. Exp Dermatol. 2011; 20(7):605–613. [PubMed: 21692861]
52. Cerqueira MT, Pirraco RP, Santos TC, Rodrigues DB, Frias AM, Martins AR, Reis RL, Marques AP. Human adipose stem cells cell sheet constructs impact epidermal morphogenesis in full-thickness excisional wounds. Biomacromolecules. 2013; 14(11):3997–4008. [PubMed: 24093541]
53. Hocking AM, Gibran NS. Mesenchymal stem cells: paracrine signaling and differentiation during cutaneous wound repair. Exp Cell Res. 2010; 316(14):2213–2219. [PubMed: 20471978]
54. Walter MN, Wright KT, Fuller HR, MacNeil S, Johnson WE. Mesenchymal stem cell-conditioned medium accelerates skin wound healing: an in vitro study of fibroblast and keratinocyte scratch assays. Exp Cell Res. 2010; 316(7):1271–1281. [PubMed: 20206158]
55. Gauglitz GG, Korting HC, Pavicic T, Ruzicka T, Jeschke MG. Hypertrophic scarring and keloids: pathomechanisms and current and emerging treatment strategies. Mol Med. 2011; 17(1–2):113–125. [PubMed: 20927486]
56. Fathke C, Wilson L, Hutter J, Kapoor V, Smith A, Hocking A. Contribution of bone marrow-derived cells to skin: collagen deposition and wound repair. Stem Cells. 2004; 22(5):812–822. [PubMed: 15342945]
57. Pradhan L, Andersen ND, Nabzdyk3 C, LoGerfo FW, Veves A. Wound-healing abnormalities in diabetes and new therapeutic interventions. US Endocrinol. 2007; 1:68–72.
58. Galiano RD, Tepper OM, Pelo CR, Bhatt KA, Callaghan M, Bastidas N, Bunting S, Steinmetz HG, Gurtner GC. Topical vascular endothelial growth factor accelerates diabetic wound healing through increased angiogenesis and by mobilizing and recruiting bone marrow-derived cells. Am J Pathol. 2004; 164(6):1935–1947. [PubMed: 15161630]
59. Zhou K, Ma Y, Brogan MS. Chronic and non-healing wounds: the story of vascular endothelial growth factor. Med Hypotheses. 2015; 85(4):399–404. [PubMed: 26138626]
60. Nomi M, Atala A, Coppi PD, Soker S. Principals of neovascularization for tissue engineering. Mol Aspects Med. 2002; 23(6):463–483. [PubMed: 12385748]
61. Jakobsson L, Franco CA, Bentley K, Collins RT, Ponsioen B, Aspalter IM, Rosewell I, Busse M, Thurston G, Medvinsky A, Schulte-Merker S, Gerhardt H. Endothelial cells dynamically compete for the tip cell position during angiogenic sprouting. Nat Cell Biol. 2010; 12(10):943–953. [PubMed: 20871601]
62. Shohara R, Yamamoto A, Takikawa S, Iwase A, Hibi H, Kikkawa F, Ueda M. Mesenchymal stromal cells of human umbilical cord Wharton's jelly accelerate wound healing by paracrine mechanisms. Cytotherapy. 2012; 14(10):1171–1181. [PubMed: 22900957]

63. Iozzo RV, Cohen IR, Grassel S, Murdoch AD. The biology of perlecan: the multifaceted heparan sulphate proteoglycan of basement membranes and pericellular matrices. Biochem J. 1994; 302(Pt 3):625–639. [PubMed: 7945186]

64. Kusuma S, Peijnenburg E, Patel P, Gerecht S. Low oxygen tension enhances endothelial fate of human pluripotent stem cells. Arterioscler Thromb Vasc Biol. 2014; 34(4):913–920. [PubMed: 24526696]

65. Tsang WP, Shu Y, Kwok PL, Zhang F, Lee KK, Tang MK, Li G, Chan KM, Chan WY, Wan C. CD146+ human umbilical cord perivascular cells maintain stemness under hypoxia and as a cell source for skeletal regeneration. PLoS ONE. 2013; 8(10):e76153. [PubMed: 24204598]

66. Barrientos S, Stojadinovic O, Golinko MS, Brem H, Tomic-Canic M. Growth factors and cytokines in wound healing. Wound Repair Regen. 2008; 16(5):585–601. [PubMed: 19128254]

67. Rustad KC, Wong VW, Sorkin M, Glotzbach JP, Major MR, Rajadas J. Enhancement of mesenchymal stem cell angiogenic capacity and stemness by a biomimetic hydrogel scaffold. Biomaterials. 2012; 33(1):80–90. [PubMed: 21963148]

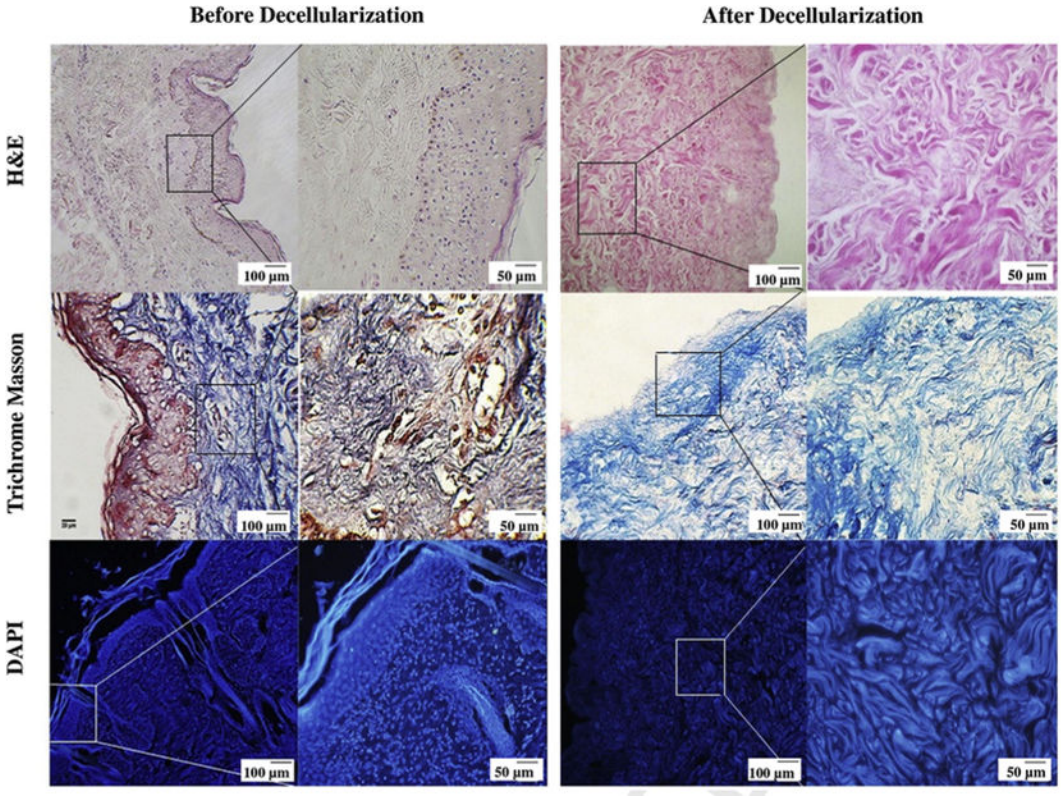

Fig. 1.

Histological assessment of human dermis before and after decellularization. H&E and Masson's trichrome staining demonstrate that there are no cells or cellular debris and skin appendages (hair follicles, sweat glands, endocrine glands etc.) in DDM following the decellularization process. The DAPI staining shows that the DDM scaffold is free of cellular nuclei, while it retains structural integrity during processing. The Masson's trichrome stained light micrographs illustrate that the DDM scaffolds preserved the normal collagen bundling pattern and normal collagen orientation.

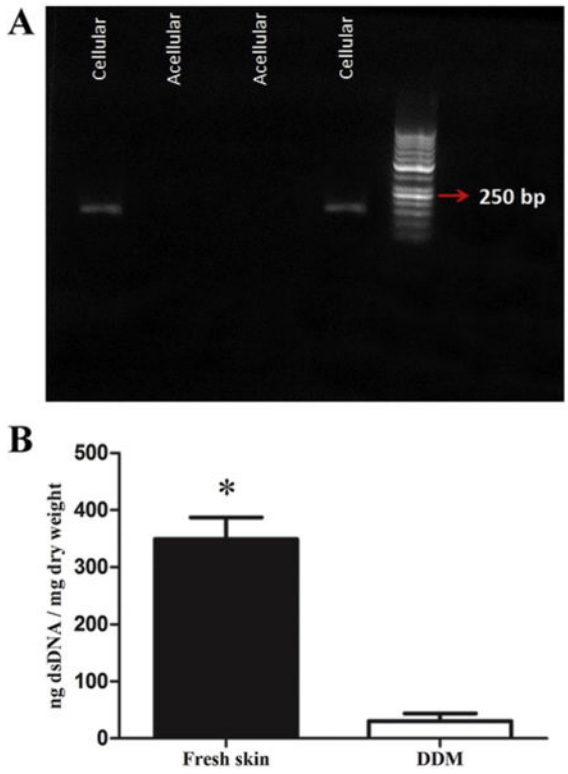

Fig. 2.

The effect of decellularization process on DNA content. (A) The PCR fragments in the fresh skin and DDM scaffolds identified by agarose gel electrophoresis. The red arrow shows the 250 kb band in the standard ladder. The PCR analysis illustrated that the samples had no detectable copies of β-actin. (B) The dsDNA concentration of the fresh skin and DDM were determined by using a Quanti-iT PicroGreen® dsDNA assay. The dsDNA concentration significantly decreased in the DDM scaffolds after processing (*P<0.001). Points are means ± SD. (For interpretation of the references to colour in this figure legend, the reader is referred to the web version of this article.)

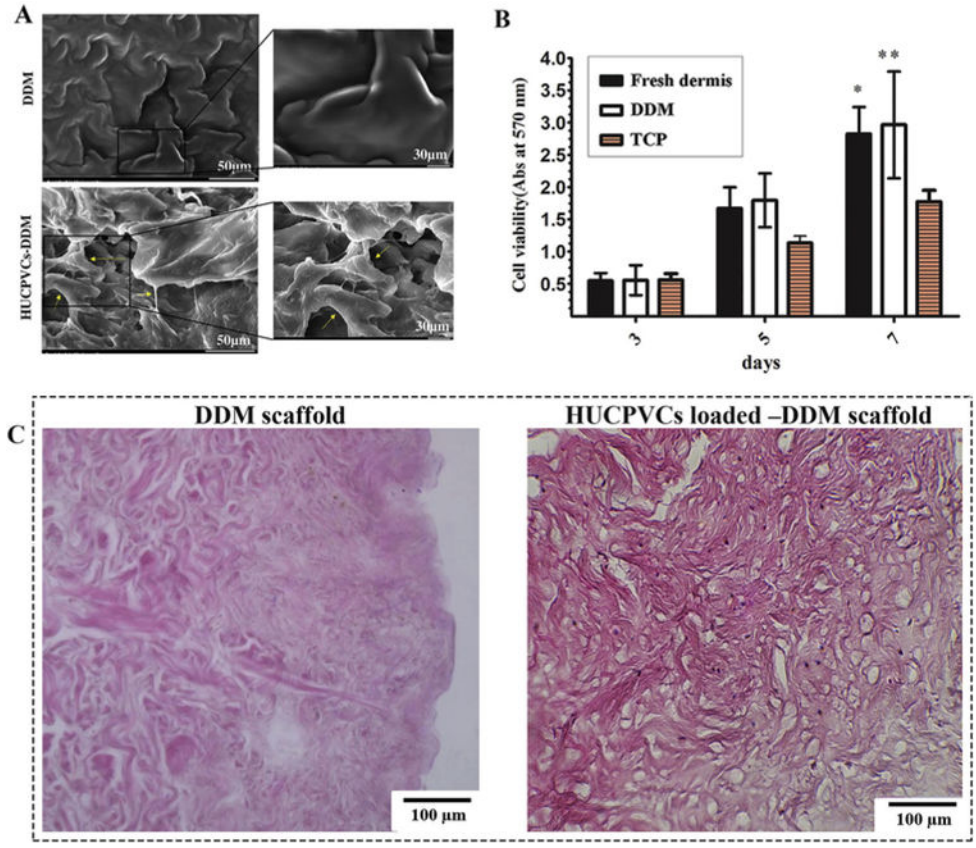

Fig. 3.

Cellular interaction of the DDM scaffolds with HUCPVCs. (A) Representative SEM micrographs of the DDM scaffold showing that the HUCPVCs cells were attached and distributed on the surface of the scaffolds after 5 days. The augmented cells attached to each other and to the surface of the DDM scaffolds. The extended lamellipodia of the HUCPVCs can be observed in the DDM scaffolds. (B) The MTT photograph revealed that there was a significant difference between the experimental groups and control group after 7 days. These results suggested that the DDM scaffolds promoted the HUCPVCs proliferation and had no cytotoxic effects. (*P* values of the fresh dermis group and DDM group are $*P < 0.05$, $**P < 0.01$ respectively). (C) Histological evaluation of DDM scaffold and HUCPVCs loaded–DDM scaffold after 7 days *in vitro* culture.

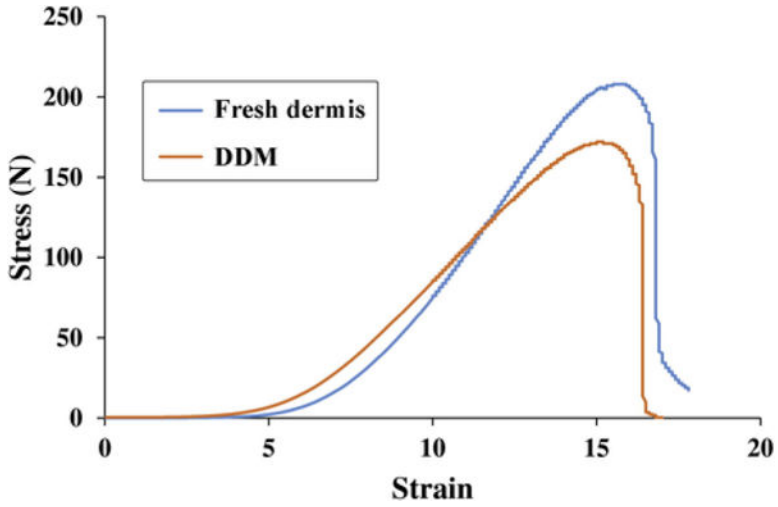

Fig. 4.

Tensile strength of the DDM scaffolds. The results of uniaxial tensile testing showed no significant differences under the conditions tested. For the fresh dermis and DDM scaffolds of similar thickness, the ultimate tensile strength (UTS) of the fresh dermis was approximately 0.77 Mpa greater than the DDM scaffolds, which was not a statistically significant difference. The breakdown pattern was observed to be similar between the fresh dermis and the DDM scaffolds, indicating that the DDM scaffold had strong mechanical properties similar to fresh skin.

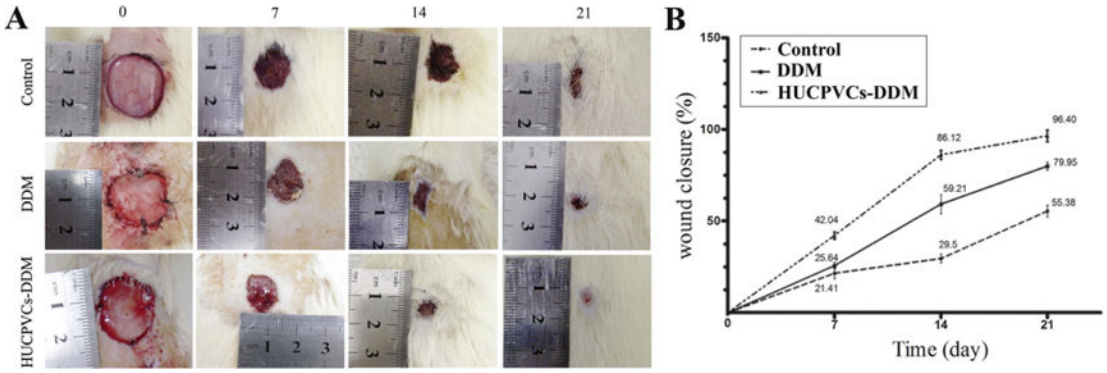

Fig. 5.

Wound healing effects of DDM alone and HUCPVCs loaded-DDM in a diabetic rat model of cutaneous wounds. (A) Representative photographs of the wound closure rate among the three groups at days 0, 7, 14 and 21 after grafting. (B) Quantitative analysis indicated that the wound size was reduced in the HUCPVCs loaded-DDM group compared with the control and DDM groups after 21 days ($P < 0.001$). The results showed that wound closure rate in the DDM group was higher than control group, and significant differences were observed at 7 and 14 days post-wounding ($P < 0.001$). The HUCPVCs loaded-DDM group demonstrated no significant improvement in wound healing compared with the DDM treated groups at 7 days. Moreover, the HUCPVCs loaded-DDM scaffolds had much higher wound healing rate and contraction ability than the other groups.

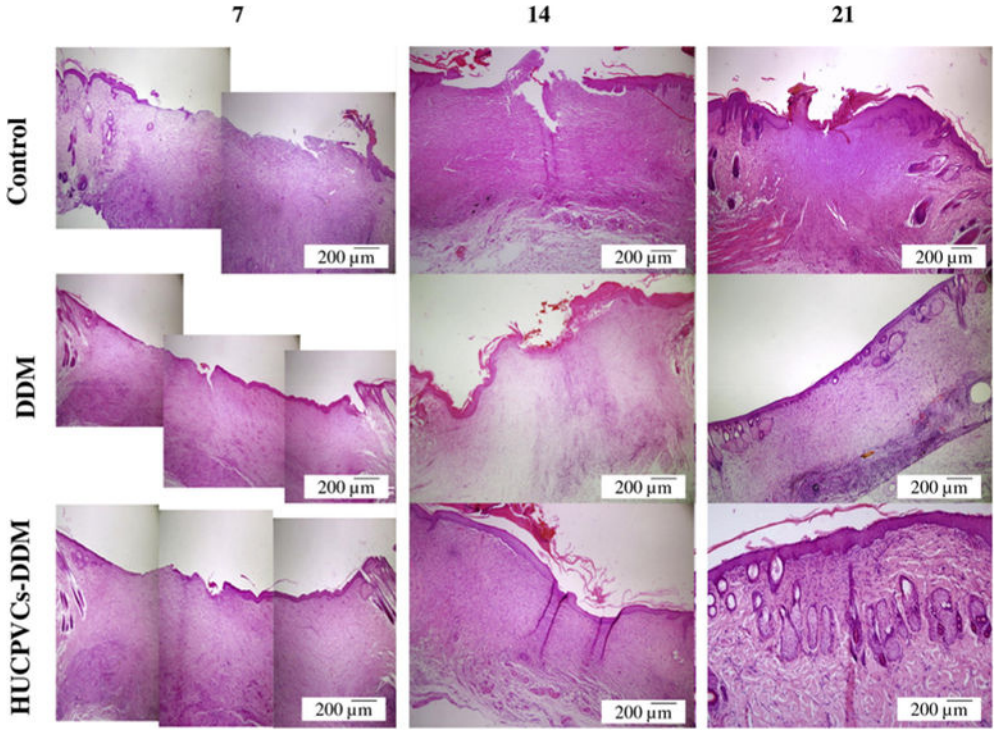

Fig. 6.

Representative photomicrographs showing the histology for the structure of epithelial and dermal layer and healing status in each group over 21 days after transplantation (H&E). After 7 days, the control, DDM and HUCPVCs loaded-DDM groups showed a number of inflammatory cells. In the HUCPVCs loaded-DDM group, some collagen fibers and fibroblasts appeared in the wound area, which related to the migration phase of wound healing process, indicating that the HUCPVCs loaded-DDM scaffold had a significant effect on the wound healing process compared with other groups. The moderate inflammation remained in the control group until 14 days. The results also show that the epidermal layer was completely formed in the HUCPVCs loaded-DDM group and covered the entire wound site after 2 weeks. However, the re-epithelization process was slow in the other groups. The HUCPVCs loaded-DDM group showed better wound healing compared with the control and DDM groups, demonstrating no sign of immunorejection over 21 days post transplantation.

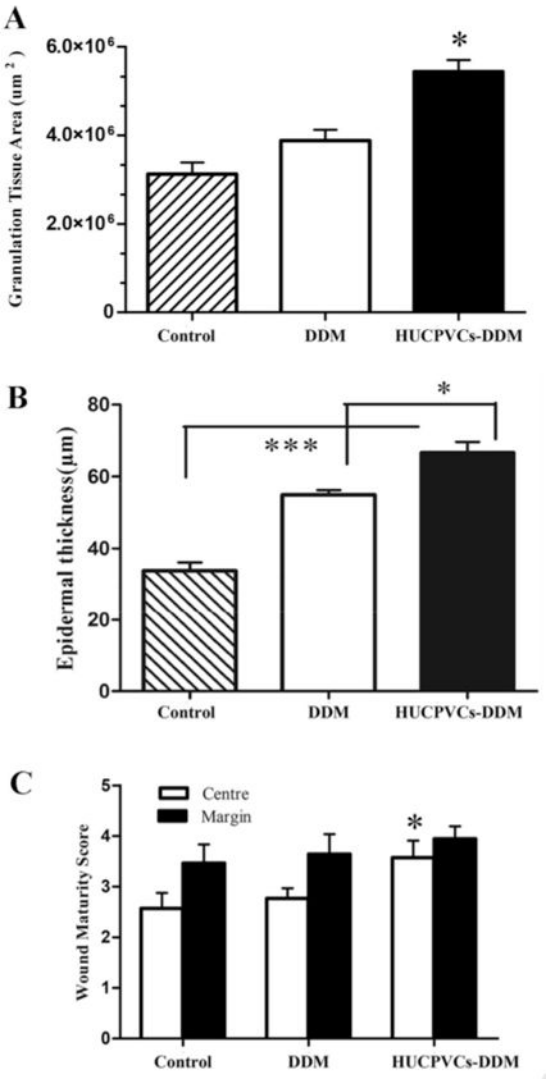

Fig. 7.

Formation of granulation tissue, epidermal thickness and wound maturity. (A) Area of granulation tissue of wounds treated with the HUCPVCs loaded-DDM scaffold were much higher than DDM and control groups (*$P < 0.001$). (B) The HUCPVCs-loaded DDM scaffold treated wounds demonstrated an increased thickness of the newly regenerated epidermis compared with the other groups at 7 days (*$P < 0.001$, ***$P < 0.0001$). Furthermore, the epithermal layer thickness in the DDM scaffold treated groups was significantly higher than control group (***$P < 0.0001$). (C) Wound maturity was measured in margin and central parts of different implanted groups, showing that the wound maturity was significantly higher in the HUCPVCs loaded-DDM treated group, especially in the central part of the wound site compared to DDM and control groups (*$P < 0.001$).

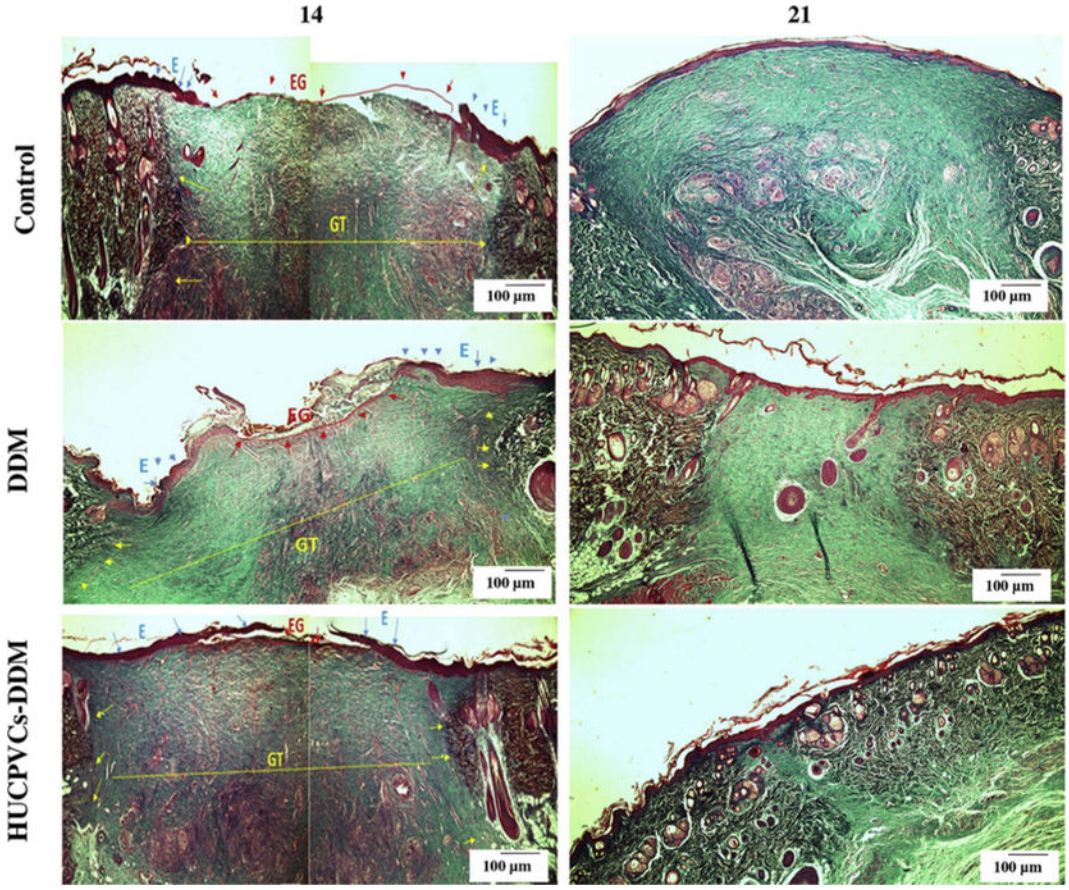

Fig. 8.

Masson's trichrome staining of the control, DDM and HUCPVCs-DDM groups at 14 and 21 days post implantation. The collagen bundles started to appear in the wound treated with DDM and HUCPVCs-loaded DDM scaffolds after 14 days, after which a better remodeling progress was observed for the HUCPVCs-loaded DDM scaffolds. However, more collagen accumulation and deposition was observed in the control group after 21 days.

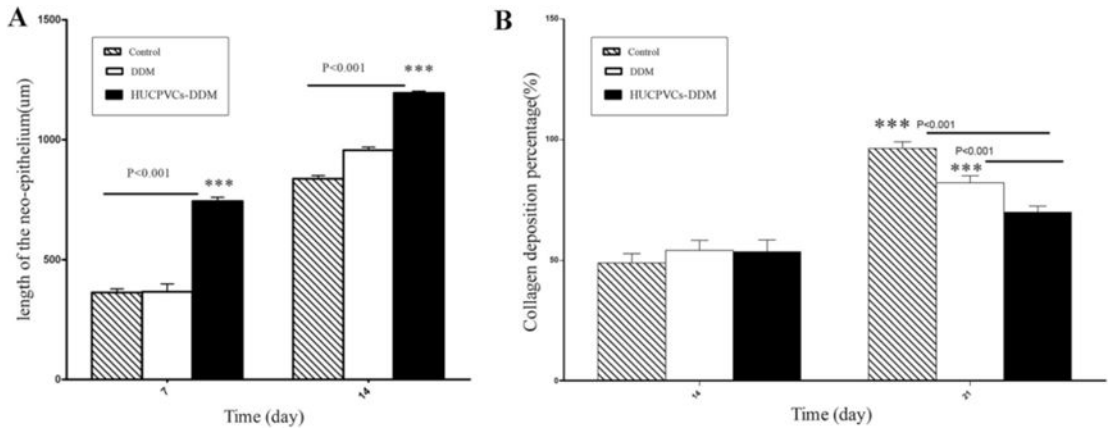

Fig. 9.

(A) The length of the newly formed epithelium measured in three groups at days 7 and 14, indicating that the length of the neo-epithelium was statically significant in the HUCPVCs-loaded DDM group compared with that of DDM and control groups after 14 days ($P < 0.001$). While there was no significant difference between the DDM and control groups. (B) The measurement of the percentage of collagen deposition was higher in control groups after 21 days ($P < 0.001$). There was no significant difference between all the groups at day 14. (E, EG and GT refer to epithelization, epithelial gap and granulation tissue, respectively.).

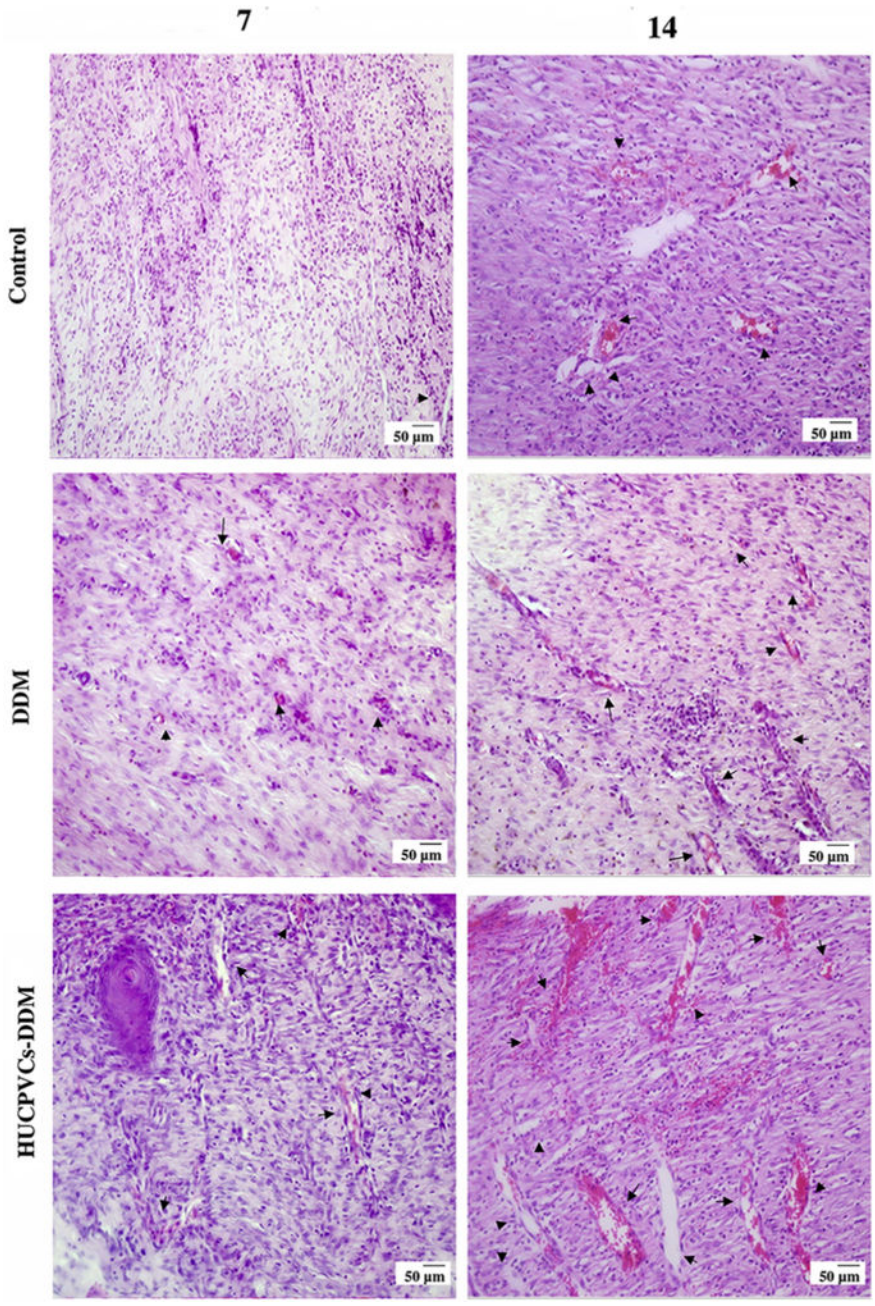

Fig. 10.

The angiogenic effect of DDM and HUCPVCs-loaded DDM scaffolds in diabetic wounds are shown in H&E sections. The sections clearly show blood vessels (black arrows) in the control, DDM and HUCPVCs-DDM scaffolds treated groups. In addition, the capillary density increased in the HUCPVCs loaded-DDM scaffold treated group.

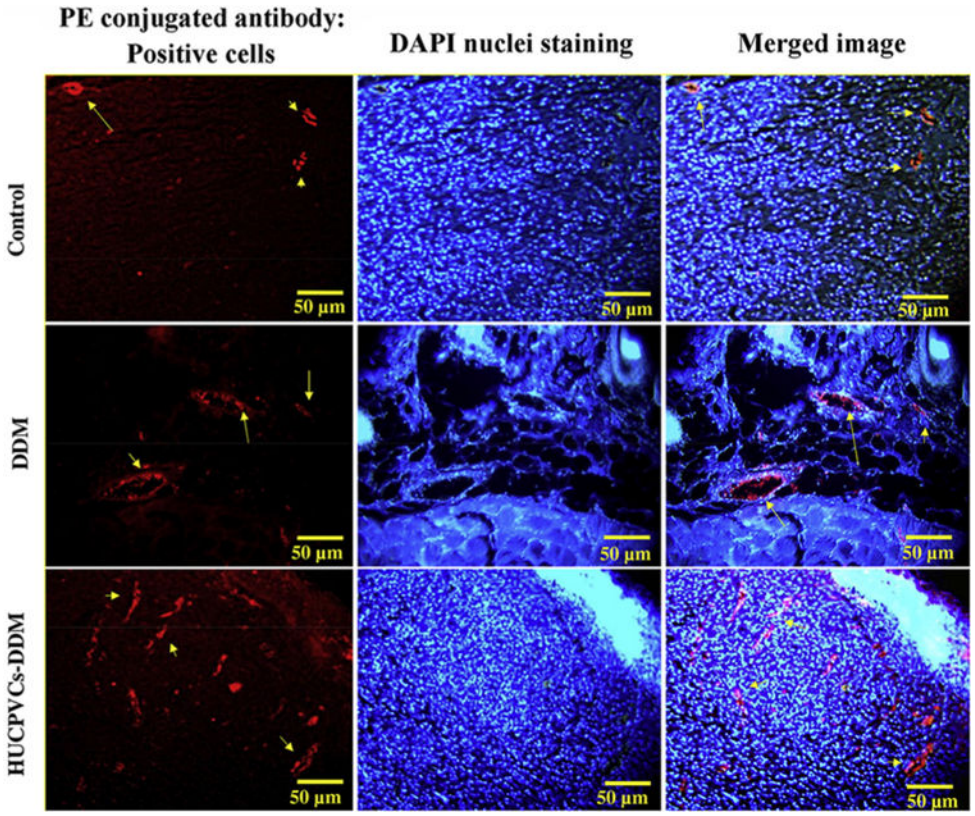

Fig. 11.

The angiogenesis activity of the scaffolds were detected by immunofluroscence staining for VEGFR-2 expression (red) in wound tissue are shown for different groups at the day 7 post implantation. The HUCPVCs-loaded DDM group showed a higher number of VEGFR-2-positive endothelial cells. (PE refers to phycoerythrin). (For interpretation of the references to colour in this figure legend, the reader is referred to the web version of this article.)

Table 1

The characteristic of primers used for real-time RT-PCR assays.

Accession number	Targetgene	Primer sequence	Product size (bp)
NM-001101.3	β-Actin	Forward: 5′TCAGAGCAAGAGAGGCATCC3′	187
		Reverse: 5′GGTCATCTTCTCCACGGTTGG3′	

Table 2

Tensile test results of fresh skin and DDM scaffold (mean ± SD).

	Fresh dermis	DDM (Decellularized dermis)
Maximum load (N)	207 ± 5.04	167 ± 3.21
Tensile strength (Mpa)	14.47 ± 0.18	13.7 ± 0.26
E –Modulus (Mpa)	24.39 ± 0.46	21.15 ± 0.26

Student‘s *t* test; fresh skin versus ADM scaffold. No significant difference.